

Chemical Reactivity Controlled by Negative Hyperconjugation: A Theoretical Study

Sten O. Nilsson Lill,^[a] Guntram Rauhut,^[b] and Ernst Anders*^[a]

Abstract: Negative hyperconjugation is a general phenomenon that can be observed in many areas of chemistry. The knowledge of its impact on structural parameters and conformational issues is well established, but little is known about its importance for chemical reactivity. Here we present a systematic study of different aspects of negative hyperconjugation on the reactivity

of complex heterocyclic systems using density functional theory. Intermediates from the reaction of nitrogen-based nucleophiles with bis(1,3,4-thiadiazolo)-

1,3,5-triazinium halides serve as benchmark systems to demonstrate the effects of negative hyperconjugation on bond lengths, on the relative stability of conformational isomers and transition structures and, most importantly, on the different reaction pathways of these species. The computational results provided here are in part supported by experiments reported elsewhere.

Keywords: conformation analysis • density functional calculations • heterocycles • hyperconjugation • NBO analysis

Introduction

Chemical reactivity controlled by stereoelectronic effects is a topic of much current interest.^[1–9] The most classical example involving stereoelectronic effects is the “anomeric effect”,^[10, 11] which explains the thermodynamic preference of an electronegative substituent to occupy the axial rather than the equatorial position at the anomeric carbon of a glycopyranosyl derivative. The origin of the anomeric effect was for long debated, but it is now clear that the major contribution comes from negative hyperconjugation in which a heteroatom lone pair interacts with σ^* orbitals. Negative hyperconjugation has been shown to be a general chemical phenomenon that also influences the thermodynamic stabilities of conformers of 1,3-dioxanes,^[12] 1,3-dithianes,^[13] phosphoryl anions,^[14] tetrahydropyranes^[7, 15] and acetals,^[16] halogenated alkyl anions and halogenated alkylamines^[17, 18] or diazenes.^[19] In the same context, hyperconjugation, that is, electron delocalisation from σ orbitals into vacant π^* orbitals, has been shown to, for example, dictate conformational stabilities

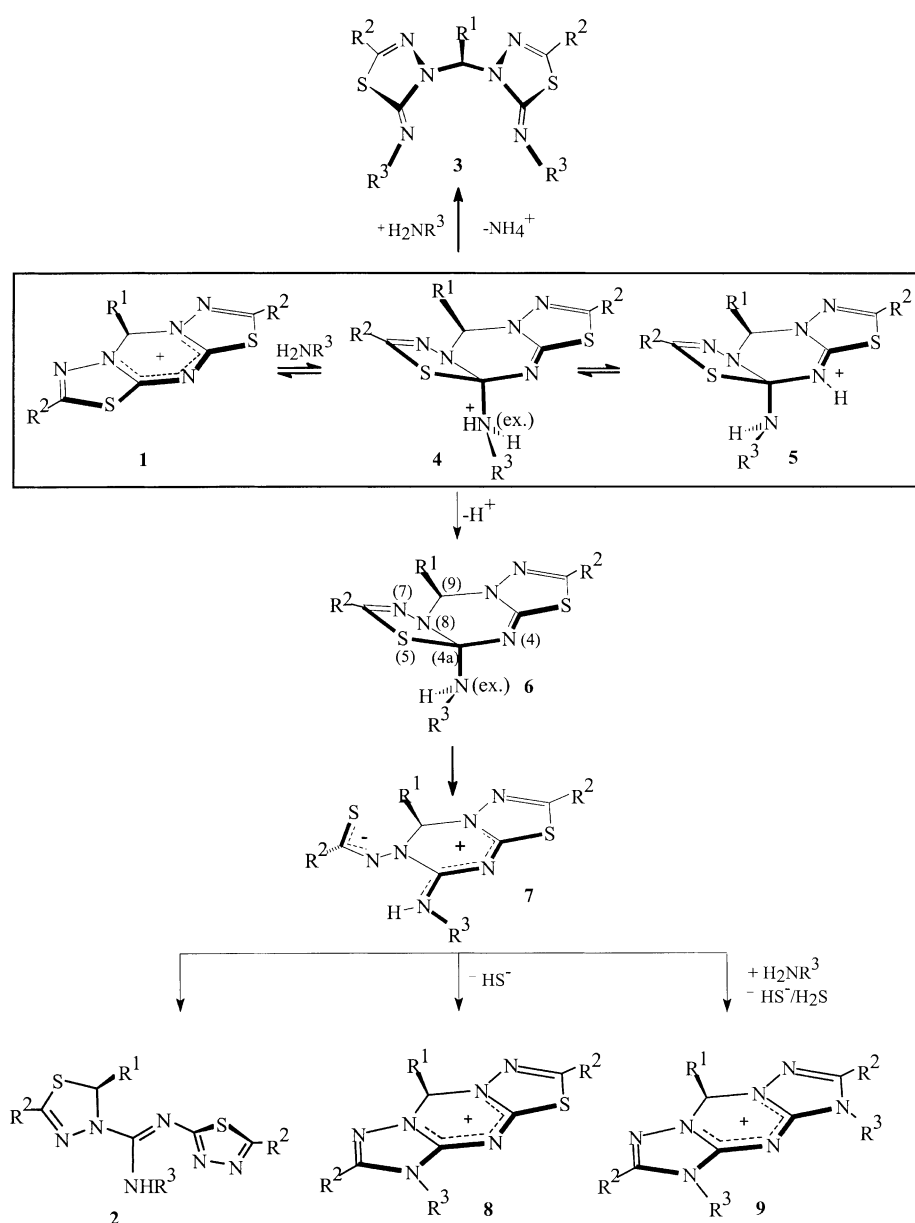
of the phosphodiester backbone of nucleosides^[20] and determine stabilities of rotational isomers of alkanes.^[21, 22] Regarding chemical reactivity, the kinetic anomeric effect refers to when a heteroatom lone pair in the transition state (TS) interacts with an acceptor σ^* orbital. In order to maximise the interaction, the lone pair and the σ^* orbital preferably adopt an antiperiplanar orientation. The effects of negative hyperconjugation upon increased chemical reactivity have, in a few cases, been successfully characterised by computational chemistry.^[2–8] An elegant example of using negative hyperconjugative effects as a tool to control product formation has recently been presented by one of us.^[23–27] The novel formation of bis(1,3,4-thiadiazolo)-1,3,5-triazinium halides **1** and their reactions with nitrogen-based nucleophiles results in the formation of highly substituted guanidines **2** or bis(thiadiazolyl)alkanes (“aminals”) **3**.^[23, 24] These compounds are formed by two different reaction channels involving separate inter- or intramolecular proton-transfer-mediated ring-opening reactions from intermediates **4–7** shown in Scheme 1.

In intermolecular proton transfer, an external base abstracts the N(ex.) proton from **4** leading via **6** to a zwitterionic compound **7**, which can further react to give guanidines **2** or, depending on the attacking nucleophile and conditions used, to give [(1,2,4-triazolo)-(1,3,4-thiadiazolo)]-1,3,5-triazinium halides **8** or bis(1,2,4-triazolo)-1,3,5-triazinium halides **9** (Scheme 1).^[25–27] An intramolecular proton transfer from N(ex.) to N(4),^[27] generating intermediate **5**, is responsible for the formation of aminals **3**. Proton transfer from N(ex.) allows the N lone pair of **5** (or **6**) to interact with accessible electron-accepting σ^* orbitals, that is, by negative hyperconjugation. The acceptor orbitals of the intermediates

[a] Prof. Dr. E. Anders, Dr. S. O. Nilsson Lill
Institut für Organische Chemie und Makromolekulare Chemie
Friedrich-Schiller-Universität, Lessingstrasse 8
07743 Jena (Germany)
Fax: (+49)3641-948212
E-mail: ernst.anders@uni-jena.de

[b] Priv.-Doz. Dr. G. Rauhut
Institut für Theoretische Chemie, Universität Stuttgart
Pfaffenwaldring 55, 70550 Stuttgart (Germany)

Supporting information for this article is available on the WWW under <http://www.chemeurj.org/> or from the author.



Scheme 1. Formation of guanidines **2**, aminas **3**, [(1,2,4-triazolo)-(1,3,4-thiadiazolo)]-1,3,5-triazinium halides **8** or bis(1,2,4-triazolo)-1,3,5-triazinium halides **9** from the intermediates **4**–**7** generated by treating bis(1,3,4-thiadiazolo)-1,3,5-triazinium halides **1** with nitrogen-based nucleophiles.

involve the C(4a)–S(5)-, C(4a)–N(4)- and C(4a)–N(8) bonds (Scheme 1). Population of an antibonding σ^* orbital of a bond involving C(4a) will result in bond elongation. This will facilitate bond cleavage and hence ring opening and shortening of the C(4a)–N(ex.) bond. With detailed knowledge of the role of negative hyperconjugation in these systems, product formation can be controlled by this stereoelectronic effect.

The quantification of the negative hyperconjugative effect on the chemical reactivity of the uncharged model system **6** ($R^1 = R^2 = \text{H}$, $R^3 = \text{CH}_3$) and the cationic model system **5** ($R^1 = R^2 = R^3 = \text{CH}_3$)^[28] (Scheme 1) is presented here. The thermodynamic stabilities of three different isomers of these model systems, representing the three possible electron-accepting antibonding σ^* orbitals of the C(4a)–N(8)-,

C(4a)–S(5)- or C(4a)–N(4)-bonds, here denoted **A**, **B** and **C**, respectively, are computationally investigated. Natural bond orbital (NBO) analyses are performed in order to quantify the negative hyperconjugative effects in the transition states responsible for the different reaction channels.

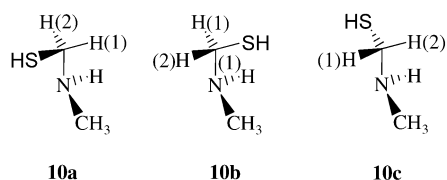
Computational Methods

All compounds were optimised by using Gaussian 98,^[29] and NBO analyses were performed by using NBO 5.0.^[30] All geometries were characterised as minima or TSs by the use of the sign of the eigenvalues of the force-constant matrix obtained from a frequency calculation. Optimised TSs with one imaginary frequency were confirmed to describe the correct displacement by a normal-mode analysis. Three different hybrid density functionals (B3LYP^[31, 32] mPW1PW91,^[33, 34] and mPW1K^[35]) were applied since it has been shown that the exchange-functional mPW1 has improved long-range behaviour compared with B3LYP. It may also represent charge-transfer complexes and weak interactions better than other density functionals.^[33] The mPW1K functional has been parameterised for reproducing activation barriers and reaction energies and gives geometries and energies with accuracy in comparison with QCISD^[36, 37] results. Some compounds in this study were also optimised with MP2^[38] or QCISD^[39] as implemented in Gaussian 98. Two different basis sets were used: Pople's 6-311++G(d,p)^[40–43] basis set and Dunning's correlation-consistent basis set aug-cc-pvdz.^[44, 45] Generally in the text, calculated zero-point energy-corrected energies and structural parameters refer to mPW1K/aug-cc-pvdz results. Calculated relative energies found

by using the hybrid density functionals can be found in the Supporting Information. Reaction paths were identified by using IRC calculations^[46–49] for most of the rotational or inversion TSs. NBO analyses were performed to quantify the negative hyperconjugative effects.^[30, 50]

Results and Discussion

Model system methylaminomethanethiol (10): In order to assess the reliability of the different density functionals to describe negative hyperconjugative effects correctly, methylaminomethanethiol (**10**) (Scheme 2) was investigated for use as a reference system to estimate the negative hyperconjugative effects. At the mPW1K/aug-cc-pvdz level of theory, the most stable isomer of model system **10** was **10b** (Scheme 2), in



Scheme 2. Different isomers of the model system methylaminomethanethiol (**10**).

which the N lone pair was delocalised into the $\sigma^*[\text{C}(1)\text{--S}]$ orbital. As a consequence, the C(1)–S bond length was found to be 1.853 Å. In isomers **10a** and **10c**, the lone pair delocalises into a $\sigma^*[\text{C}(1)\text{--H}]$ orbital. These isomers are calculated to be 3.2 and 2.0 kcal mol⁻¹, respectively, less stable than **10b** (Table 1). In **10a** the C(1)–S bond length is computed to be 1.812 Å and in **10c** to be 1.822 Å, thus shorter than in **10b** since the N lone pair in these isomers is antiperiplanar with a C(1)–H bond rather than with the C(1)–S bond. This is also reflected in the increase in the C(1)–H bond lengths in **10a** and **10c** relative to **10b**.

The geometry effect of the lone pair– σ^* interaction can be estimated by deleting the corresponding off-diagonal element of the Fock matrix within a basis of natural orbitals, and a subsequent geometry optimisation by using the modified total energy of the molecule. For details of such procedures see ref. [50]. The impact of the negative hyperconjugation on structural parameters has thus been studied by reoptimising isomer **10b** within this approximation. In the reoptimised **10b**, a decrease in the C(1)–S bond length of 0.044 Å is detected. The C(1)–N bond is also affected by this neglect of the lone pair– σ^* interaction. The bond length changes from 1.421 Å when the negative hyperconjugation is “on”, to 1.441 Å when it is “off” (Table 1). The lone pair seeks another electron-acceptor orbital when the interaction with the $\sigma^*[\text{C}(1)\text{--S}]$ orbital is deleted. In the reoptimised **10b**, the C(1)–H(1) bond is elongated and thus is the new acceptor bond. The new minimum found is similar to isomer **10a**. Thus, there is clear evidence showing that lone pair electron delocalisation by negative hyperconjugation elongates the bond involving the σ^* orbital and shortens the C(1)–N bond. This allows for detection of negative hyperconjugation effects in compounds **5** and **6** by using these geometrical parameters.

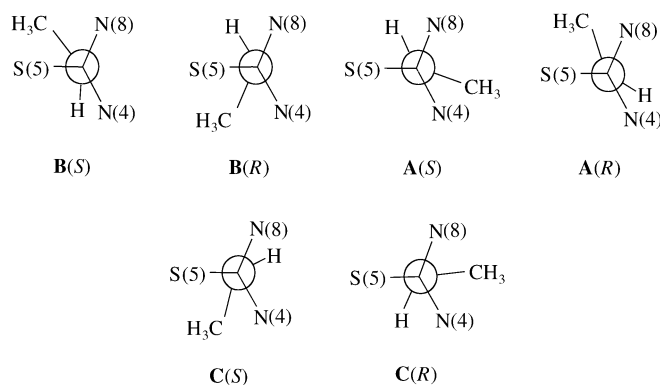
To validate the accuracy of the density functionals mPW1K and B3LYP, isomers **10a** and **10b** were also optimised at the QCISD level. From Table 1, it can be seen that both the

C(1)–S bond (1.874 Å) and the C(1)–N bond (1.447 Å) in **10b** are found to be slightly longer with QCISD than with mPW1K (1.853 Å and 1.421 Å, respectively). Similarly in **10a**, both the C(1)–S bond and the C(1)–N bond are somewhat longer according to QCISD than mPW1K. The relative energy of isomer **10a** compared with **10b** calculated at the QCISD level of theory is found to be in good comparison with that calculated with mPW1K (2.7 and 2.9 kcal mol⁻¹, respectively). This shows that the mPW1K functional is reliable in describing the effect of the lone pair– σ^* -orbital interaction regarding effects on geometries and energies, and thus is valid to use for studying the effects of negative hyperconjugation.

The relative energy of **10a** compared with **10b** calculated by using B3LYP is slightly higher than that calculated by using QCISD or mPW1K (Table 1). Furthermore, the difference in the C(1)–S bond length between **10a** and **10b** is larger with B3LYP (0.057 Å) than that observed for QCISD (0.037 Å) or mPW1K (0.041 Å). This might indicate that B3LYP overestimates the effect of the negative hyperconjugation in comparison with QCISD and mPW1K.

Uncharged model compound 6: In this section, the thermodynamic stabilities of different isomers of **6** ($\text{R}^1 = \text{R}^2 = \text{H}$; $\text{R}^3 = \text{CH}_3$, Scheme 1) are presented. The investigated isomers denoted **A**, **B** and **C** involve the N(ex.)-lone pair interaction with the antibonding σ^* orbitals of the C(4a)–N(8)-, C(4a)–S(5)- and C(4a)–N(4) bond, respectively.

The most stable isomer of model compound **6** was found to be **6B(S)** (Schemes 3 and 4), in which the lone pair of N(ex.) is

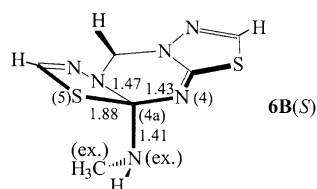


Scheme 3. Newman projection along the C(4a)–N(ex.) bond of the **A**, **B** and **C** isomers of **5** and **6**.

Table 1. Calculated relative energies ΔE [kcal mol⁻¹] and bond lengths [Å] of isomers of the model compound **10**.

Isomer	Method	$\Delta E/\Delta E_{\text{ZPE}}^{[a]}$	Bond			
			C(1)–S	C(1)–H(2)	C(1)–H(1)	C(1)–N
10a	i) mPW1K/aug-cc-pvdz	3.22/2.90	1.812	1.093	1.099	1.437
	ii) B3LYP/6-311++G(d,p)	3.87/3.52	1.836	1.093	1.100	1.451
	iii) QCISD/aug-cc-pvdz	3.00/2.67	1.837	1.103	1.109	1.463
10b	i)	0	1.853	1.091	1.091	1.421
	i) ^[b]	–	1.809 ^[b]	1.093 ^[b]	1.099 ^[b]	1.441 ^[b]
	ii)	0	1.893	1.090	1.090	1.428
	iii)	0	1.874	1.100	1.101	1.447
10c	i)	2.01/1.86	1.822	1.101	1.090	1.433
	ii)	2.30/2.14	1.851	1.101	1.090	1.444

[a] Zero-point energy (ZPE) corrected relative energies. [b] Reoptimised geometry after deletion of the lone pair– $\sigma^*[\text{C}(1)\text{--S}]$ interaction.



Scheme 4. Dihedral angle $\gamma = 47^\circ$ (C(ex.)-N(ex.)-C(4a)-S(5)) in **6B(S)**, the most stable isomer.

antiperiplanar to the C(4a)–S(5) bond. This is indicated by the C–S bond elongation (1.890 Å, see Table 2) and the shortening of the C(4a)–N(ex.) bond (1.411 Å) compared with model system **10b**. Isomer **6B(R)** with inverted configuration at N(ex.) is calculated to be only 0.9 kcal mol⁻¹ higher in energy than **6B(S)** (Table 2). Its corresponding bond lengths are 1.892 Å and 1.415 Å.

The interaction of the N(ex.) lone pair with the σ^* [C(4a)–N(8)] orbital yields two possible **6A** isomers, **6A(R)** and **6A(S)** (Scheme 3). These are 3.1 and 5.4 kcal mol⁻¹, respectively, higher in energy than **6B(S)**. The C(4a)–N(8) bonds in these isomers are somewhat elongated and are 1.482 and 1.490 Å, respectively. The C(4a)–N(ex.) bonds are found to be 1.411 Å and 1.421 Å, respectively. The latter C–N-bond shortening, relative to isomer **10b**, indicates the presence of negative hyperconjugation.

The third possible pair of isomers stabilised by negative hyperconjugation is **6C(S)** and **6C(R)** (Scheme 3), in which the N(ex.) lone pair is antiperiplanar to the σ^* [C(4a)–N(4)] orbital. These isomers are calculated to be 7.5 and 8.8 kcal mol⁻¹ less stable than the most stable isomer **6B(S)**. Here, the C(4a)–N(ex.) bonds are calculated to be 1.428 and 1.438 Å, respectively. The shortest C(4a)–N(ex.) bonds of all the optimised isomers of **6** are thus found in the **6A(R)** and the **6B(S)** isomers. This indicates that the negative hyperconjugation is largest in these two isomers. The quantification of the negative hyperconjugation in the different isomers will be presented in a later section.

Table 2. Calculated bond lengths [Å], dihedral angles [°] and relative energies ΔE [kcal mol⁻¹] of isomers of the model system **6** at the mPW1K/aug-cc-pvdz level of theory.

Isomer	Bond				$\Delta E/\Delta E_{\text{ZPE}}^{[a]}$	Dihedral angle γ	Main acceptor σ^* [X–Y] bond orbital
	C(4a)–S(5)	C(4a)–N(8)	C(4a)–N(4)	C(4a)–N(ex.)			
6B(S)	1.890	1.470	1.434	1.411	0	47	C(4a)–S(5)
6B(R)	1.892	1.470	1.431	1.415	0.80/0.88	–70	C(4a)–S(5)
6A(S)	1.864	1.490	1.429	1.421	5.72/5.41	200	C(4a)–N(8)
6A(R)	1.870	1.482	1.435	1.411	3.62/3.13	72	C(4a)–N(8)
6C(S)	1.866	1.471	1.443	1.428	8.03/7.45	280	C(4a)–N(4)
6C(R)	1.860	1.478	1.441	1.438	9.03/8.83	174	C(4a)–N(4)
TS1	1.856	1.484	1.437	1.441	12.34/11.85	8	C(ex.)–H
TS2	1.872	1.472	1.441	1.436	9.74/9.50	142	C(ex.)–H
TS3	1.851	1.482	1.438	1.440	9.52/9.07	197	C(4a)–N(4)
TS4	1.868	1.480	1.436	1.446	13.09/12.60	121	C(4a)–N(4)
TS5	1.866	1.471	1.442	1.428	8.03/7.43	280	C(4a)–N(4)
TS6	1.848	1.476	1.442	1.440	8.83/8.57	–35	C(4a)–N(4)
TS7	1.884	1.481	1.435	1.398	3.80/2.82	67	C(4a)–S(5)
TS8	1.891	1.479	1.431	1.401	6.52/5.50	237	C(4a)–S(5)

[a] ZPE-corrected relative energies.

Investigation of rotational and inversion barriers for compound 6: Based upon the previous investigations, we continue the discussion in this section by presenting TSs for rotation of the amino group about the C(4)–N(ex.) bond and inversion at the N(ex.) centre, together with an analysis of the kinetic anomeric effect. All activation barriers and reaction energies presented are relative to the most stable isomer **6B(S)**.

In the **6B(R)** isomer, the dihedral angle γ (cf. Scheme 4) is optimised to approximately -70° (Table 2). Clockwise rotation of the amino group leads to a TS (**TS1**) that is 11.9 kcal mol⁻¹ higher in energy than **6B(S)** at the mPW1K/aug-cc-pvdz level of theory (Figure 1).

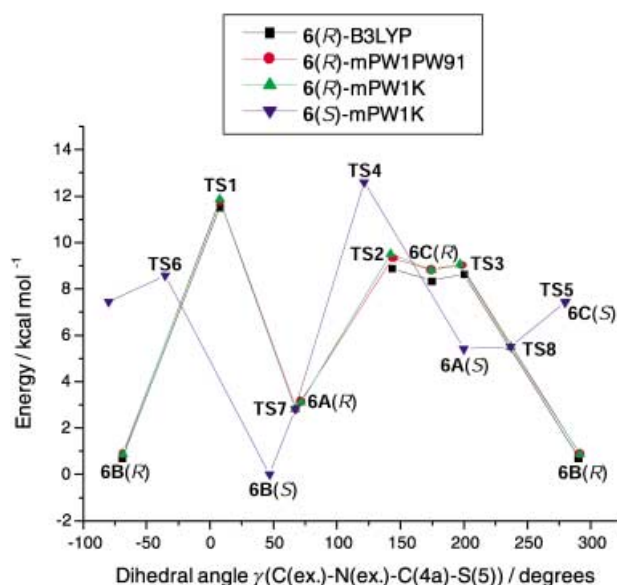


Figure 1. DFT-calculated ZPE-corrected energy profiles for compound **6**. mPW1K/aug-cc-pvdz profiles are marked with bolder lines.

Further rotation of the amino group leads to isomer **6A(R)**. Due to a very flat potential-energy surface (PES) and a nearly lying TS (**TS7**) for inversion at the N(ex.) centre, *isomer 6A(R) could only be detected by using the functionals*

mPW1PW91 or *mPW1K*. Attempts to optimise the **6A(R)** isomer at B3LYP level of theory always failed leading to isomer **6B(S)**.

At the *mPW1K* level of theory, the **6A(R)** isomer is 3.1 kcal mol⁻¹ less stable than the **6B(S)** isomer, and the inversion from **6A(R)** via **TS7** is found to be a barrierless process. Further rotation of the amino group leads to **TS2**, the rotational TS connecting the **6A(R)** and **6C(R)** isomers. The **6C(R)** isomer, found after continued rotation, is a very weak minimum as both **TS3**, the rotational TS leading back to **6B(R)** from the **6C(R)** isomer, and **TS2** are close in energy (see Table 2).

Clockwise rotation of the amino group starting from the **6B(S)** isomer leading to **6A(S)** is an endothermic process (Figure 1). The activation barrier for rotation via **TS4** is calculated to be 12.6 kcal mol⁻¹ while the activation barrier for inversion from **6B(R)** to **6A(S)** via **TS8** is found to be 5.5 kcal mol⁻¹. The inversion process from **6A(S)** is thus computed to be essentially barrierless. The **6C(S)** isomer is found to be 7.5 kcal mol⁻¹ less stable than the **6B(S)** isomer. This could *only be optimised by using the mPW1K functional or MP2*, while use of B3LYP or *mPW1PW91* always led to inversion to **6B(R)** or rotation to **6B(S)** or **6A(S)**. **TS5**, the rotational TS connecting **6A(S)** and **6C(S)**, is almost identical in energy to **6C(S)**, that is, the PES in the vicinity of **6C(S)** is extremely flat. The rotational TS **TS6** connecting **6C(S)** and **6B(S)** closes the rotational cycle. In all rotational TSs except in **TS6**, steric interactions between the proton at C(9) and either the proton at N(ex.) (**TS1** and **TS5**) or a proton in the exocyclic methyl group (**TS2–TS4**) have been discovered.^[51]

Due to the essentially barrierless inversion processes, the two **6A** isomers easily convert into **6B** isomers and, due to low rotational barriers, the two **6C** isomers can also be converted to **6B** isomers with small energy costs. This means that the population of the **6A**- and **6C** isomers is always small. Interestingly, due to the inversion processes detected at N(ex.), isomer **6A(R)** will be formed from **6B(S)** rather than by amino-group rotation from **6B(R)** (see Figure 1). Similarly, **6A(S)** will be formed from **6B(R)** rather than from **6B(S)**. Thus, the rate-determining TS found for connecting all six stable isomers is **TS3**, which has a ZPE (zero-point energy) corrected activation barrier of 9.1 kcal mol⁻¹. As is seen from Table 2 and in the Supporting Information, relative energies between the stable isomers and TSs are not significantly different with any of the different DFT functionals or calculated with the different basis sets aug-cc-pvdz or 6-311++G(d,p). Only the *mPW1K* functional could locate all stationary points on the PES.

In the TSs for inversion, the C(4a)–N(ex.) bonds are found to be very short (1.398 Å and 1.401 Å in **TS7** and **TS8**, respectively) in comparison with isomer **10b**. This indicates a strong negative hyperconjugative effect from the N(ex.) lone pair. The N(ex.) centre in these TSs has a sp^{1.7} hybridisation while the C(4a) centre is sp^{2.5} hybridised and the inversion at N(ex.) can hence take place more easily. In comparison, the N(ex.) atoms in the stable isomers **6A–6C** have hybridisations between sp^{1.9} and sp^{2.1}, and C(4a) atoms are sp^{2.6} hybridised. In **TS7**, the lone pair interacts with both the σ*[C(4a)–S(5)]- and the σ*[C(4a)–N(8)] orbitals as is evident

from the elongated bond lengths (see Table 2). The C(4a)–N(4) bonds in **TS7** and **TS8** are also elongated and thus act as electron acceptors. Clearly, this is evidence of a kinetic anomeric effect that reduces the activation barriers for inversion. Among the rotational TSs, the least stable (**TS4**) has the longest C(4a)–N(ex.) bond (see Table 2). The shortest C(4a)–N(ex.) bond is found in **TS5**, which has the lowest activation barrier and thus is the most stabilised by the kinetic anomeric effect. Quantification of the kinetic anomeric effect is elucidated by NBO analyses and is presented in the next section.

NBO-analysis of uncharged compound 6: To quantify the effect of the negative hyperconjugation, NBO analyses were performed on the optimised compounds.^[50] This allows for a detailed analysis of the contributing orbitals. Two different energies were used in the quantification: a) E_{del} , the energy change upon deletion of a specific off-diagonal element of the Fock matrix and recomputation of the energy^[50] and b) $E(2)$, a second-order perturbation approach estimating the interaction energy between the orbitals.^[53] Alabugin and Zeidan have recently found a linear relationship between E_{del} and $E(2)$.^[54] This is also found in this study. Only the most significant contributions are discussed in the text and summarised in Table 3. A detailed description is found in the Supporting Information.

In isomer **6B(S)**, the lone pair of N(ex.) is, according to the NBO analysis, mainly interacting with the antiperiplanar σ*[C(4a)–S(5)] orbital as discussed in the previous section. In addition, it is found that the lone pair also interacts with other σ* orbitals, but to a smaller extent. The occupancy number of the lone pair is calculated to be 1.86, that is, 0.14 electrons are occupying antibonding orbitals. Deletion of the interaction between the N(ex.) lone pair and the σ*[C(4a)–S(5)] orbital increases the occupancy number of the lone pair to 1.92 electrons while the occupancy number of the σ* orbital decreases from 0.12 to 0.05 electrons; this evidences the dominating direction of the negative hyperconjugation. The energy change upon the interaction deletion is 19.3 kcal mol⁻¹ (E_{del} , Table 3). The interaction energy is dependent on both the energy gap between the N(ex.) lone pair and the σ* orbital, and the magnitude of the Fock matrix element, which is proportional to the overlap matrix element.^[53, 54] The smallest energy gap between N(ex.) and the σ*[C(4a)–S(5)] orbital is found in the **6B(S)** and **6A(R)** isomers; in **6A** it is due to an elevated orbital energy of the lone pair, while in **6B** it is rather an effect of lowering of the σ* orbital (see Supporting Information for details). However, in the **6A** isomer the Fock matrix element (not shown) is smaller than in **6B**; this results in a smaller interaction energy (Table 3).

In the **6A** isomers, the N(ex.) lone pair interacts mainly with the σ*[C(4a)–N(8)] orbital, as was also inferred from the C(4a)–N(8) bond elongation. In addition, it interacts with the σ*[C(ex.)–H] and the σ*[C(4a)–S(5)] orbitals.^[55] The occupancy numbers of the N(ex.) lone pairs are calculated to be larger than in isomer **6B(S)**. Deletion of the lone pair–σ*[C(4a)–N(8)] orbital interaction results in an increased occupancy number of the lone pair and a decrease in the occupancy number of the σ* orbital as expected. The smallest

Table 3. Deletion energies^[a] (E_{del}) [kcal mol⁻¹], second-order perturbation energies ($E(2)$) [kcal mol⁻¹] and occupancy numbers (Occ.) [electrons] obtained from NBO analyses of isomers of compound **6** at the mPW1K/aug-cc-pvdz level of theory.

Isomer	$\sigma^*[\text{C}(4\text{a})-\text{S}(5)]$		$\sigma^*[\text{C}(4\text{a})-\text{N}(8)]$		$\sigma^*[\text{C}(4\text{a})-\text{N}(4)]$		$\sigma^*[\text{C}(\text{ex.})-\text{H}]$		N(ex.) lone pair Occ.	Sum of interactions $\Sigma E(2)$
	E_{del}	$E(2)$	E_{del}	$E(2)$	E_{del}	$E(2)$	E_{del}	$E(2)$		
6B(S)	19.26	22.73	5.31	6.47	–	0.53	8.74	8.65	1.860	44.97
6B(R)	18.94	21.92	2.35	2.84	–	1.80	8.61	8.41	1.871	40.84
6A(S)	4.93	6.15	14.39	17.12	–	< 0.5	10.15	9.95	1.883	40.56
6A(R)	7.65	9.64	14.44	17.32	–	< 0.5	9.72	9.67	1.870	44.70
6C(S)	4.92	5.99	–	< 0.5	12.46	13.98	9.18	8.92	1.900	35.50
6C(R)	–	1.88	–	2.23	12.21	13.37	9.49	9.09	1.908	34.05
TS1	2.41	2.96	5.78	6.97	8.04	9.08	9.47	9.16	1.909	35.95
TS2	6.62	7.97	–	< 0.5	7.88	8.92	10.06	9.73	1.896	33.73
TS3	–	< 0.5	5.98	7.16	11.42	12.82	9.09	8.81	1.905	36.12
TS4	–	4.11	–	5.86	–	9.90	–	9.32	1.903	36.68
TS5	–	6.11	–	< 0.5	–	13.93	–	8.93	1.899	35.58
TS6	–	< 0.5	–	7.86	–	9.57	–	8.48	1.908	33.89
TS7	12.73	16.51	13.13	16.31	–	< 0.5	9.55	9.72	1.847	51.92
TS8	14.77	18.96	9.16	11.48	–	< 0.5	9.59	9.74	1.851	50.21

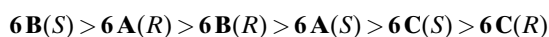
[a] The interaction between the N(ex.) lone pair and specific acceptor σ^* orbitals was deleted by use of the keyword DEL in the NBO analysis.^[50]

energy gap between the N(ex.) lone pair and the $\sigma^*[\text{C}(4\text{a})-\text{N}(8)]$ orbital among the stable isomers is found in the **6A** isomers. Although this energy gap is wider than that observed in the $\sigma^*[\text{C}(4\text{a})-\text{S}(5)]$ orbital, the interaction energy is larger due to a larger Fock matrix element.

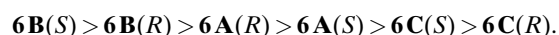
In isomers **6C**, the lone pair of N(ex.) mainly interacts with the $\sigma^*[\text{C}(4\text{a})-\text{N}(4)]$ orbital. The occupancy number of the lone pair is calculated to be even larger than in isomers **6A** and **6B**. The energy gap between the N(ex.) lone pair and the $\sigma^*[\text{C}(4\text{a})-\text{N}(4)]$ orbital is larger than for the other σ^* orbitals discussed.

In the TSs the strongest negative hyperconjugative effects involving the N(ex.) lone pair are found in the inversion TSs. In **TS7**, the occupancy number of the lone pair of N(ex.) is 1.85, that is, 0.15 electrons occupy antibonding orbitals; this is even more than in the most stable isomer **6B(S)**. In **TS7**, $\Sigma E(2)$, that is, the estimated negative hyperconjugative effect from the N(ex.) lone pair with the different σ^* orbitals, is larger than that observed in **6B(S)**. The increased hyperconjugative effect in the inversion TSs is mainly detected to be an effect of an elevated energy of the N(ex.) lone pair (Table 3 and Supporting Information). This leads to a smaller energy gap and hence larger interaction energy. Thus, there is evidence of a strong kinetic anomeric effect that reduces the inversion barriers.

As is evident from the description above, a large number of balancing negative hyperconjugative effects are present in the different isomers and determine their final geometry and energy. From the NBO analysis it is found that the largest $\Sigma E(2)$ energies are found in isomers **6B**, in which the N(ex.) lone pair interacts with the $\sigma^*[\text{C}(4\text{a})-\text{S}(5)]$ orbital. Isomers **6A** feature a somewhat smaller effect from electron delocalisation, and the smallest estimated energy stabilisations from negative hyperconjugation are found in the two **6C** isomers. Ordering of the strength of the negative hyperconjugation ($\Sigma E(2)$) in the different isomers gives the following:



while the thermodynamic stabilities result in the following ordering:



It is found that, in general, $\Sigma E(2)$ is proportional to the calculated relative energies of the stable isomers. The only exception is isomer **6A(R)**, which is thermodynamically less stable than isomer **6B(R)**, although the hyperconjugative effect is calculated to be larger. This is probably due to a counterbalancing steric interaction between the methyl group on N(ex.) and the proton at C(9).

Cationic compound 5: In this section, thermodynamic stabilities of different isomers of model compound **5** ($\text{R}^1 = \text{R}^2 = \text{R}^3 = \text{CH}_3$, Scheme 1) are presented. It has previously been shown that protonation of N(4) gives the most stable tautomer.^[27]

Among the different isomers, **5B(S)**, in which the N(ex.) lone pair is antiperiplanar to the C(4a)–S(5) bond, was found to be the most stable (Scheme 3 and Table 4). Isomer **5B(R)** is calculated to be almost isoenergetic with **5B(S)**. The C(4a)–S(5) bond length in **5B(S)** is found to be somewhat shorter than that calculated for **6B(S)**. The C(4a)–N(ex.) bonds in the **5B** isomers are also found to be shorter than in the **6B** isomers.

The isomers **5A(S)** and **5A(R)** are calculated to be 4.6 and 2.2 kcal mol⁻¹ less stable than **5B(S)**, respectively. Thus, when compound **5** is compared with compound **6**, the **A** isomers are more stabilised than the **B** isomers. In the **5A** isomers, the C(4a)–N(8) bonds are found to be shorter than in the uncharged isomers. The **5C(S)** isomer is 6.8 kcal mol⁻¹ less stable than isomer **5B(S)** and the C(4a)–N(4) bond elongation (1.526 Å) indicates that the negative hyperconjugative effect is very large in this isomer. This is also evidenced by the shortening of the C(4a)–N(ex.) bond (1.400 Å). Although the negative hyperconjugation in **5C(S)** is large, this isomer is still thermodynamically less stable than both **5B** and **5A**. Relatively speaking, the **C** isomer is also more stabilised than the **B**

Table 4. Calculated bond lengths [\AA], dihedral angles [$^\circ$] and relative energies ΔE [kcal mol^{-1}] of isomers of the model compound **5** at the mPW1K/aug-cc-pvdz level of theory.

Isomer	Bond				Dihedral angle γ	$\Delta E/\Delta E_{\text{ZPE}}$	Main acceptor $\sigma^*[\text{X}-\text{Y}]$ bond orbital
	C(4a)–S(5)	C(4a)–N(8)	C(4a)–N(4)	C(4a)–N(ex.)			
5B(S)	1.851	1.442	1.485	1.404	50	0	C(4a)–S(5)
5B(R)	1.850	1.440	1.486	1.406	–63	0.37/0.51	C(4a)–S(5)
5A(S)	1.829	1.463	1.486	1.411	178	4.55/4.58	C(4a)–N(8)
5A(R)	1.834	1.454	1.486	1.404	66	2.49/2.22	C(4a)–N(8)
5C(S)	1.829	1.440	1.526	1.400	291	7.36/6.78	C(4a)–N(4)
5C(R)	1.824 ^[a]	1.450 ^[a]	1.531 ^[a]	1.402 ^[a]	174	9.57 ^[a] /–	C(4a)–N(4)
TS21	1.824	1.450	1.503	1.417	4	8.72/8.14	C(4a)–N(4)
TS22	1.839	1.440	1.526	1.402	139	10.92/10.39	C(4a)–N(4)
TS24	1.832	1.447	1.504	1.423	118	10.21/9.78	C(4a)–N(4)
TS25	1.837	1.439	1.523	1.395	283	7.40/6.51	C(4a)–N(4)
TS26	1.816	1.446	1.515	1.412	–29	8.33/7.76	C(4a)–N(4)
TS27	1.849	1.451	1.485	1.388	61	3.16/2.27	C(4a)–N(8)
TS28	1.845	1.451	1.482	1.394	230	6.31/5.42	C(4a)–N(8)

[a] Value calculated at fixed dihedral angle.

isomers in compound **5** relative to **6**. All attempts to find the **5C(R)** isomer on the PES led to rotation to **5B(R)** or **5A(R)**, or inversion to **5B(S)**. This is probably due to a steric interaction between one of the protons of the methyl group on N(ex.) and the proton at C(9). Constraining the dihedral angle γ to that found in **6C(R)** gives an estimated relative energy of **5C(R)** compared to **5B(S)** of $9.6 \text{ kcal mol}^{-1}$.

Investigation of rotational and inversion barriers for cationic model compound 5: In this section, rotational and inversion TSs for compound **5** are presented (Figure 2). All activation barriers and reaction energies presented are relative energies compared with the most stable isomer **5B(S)**.

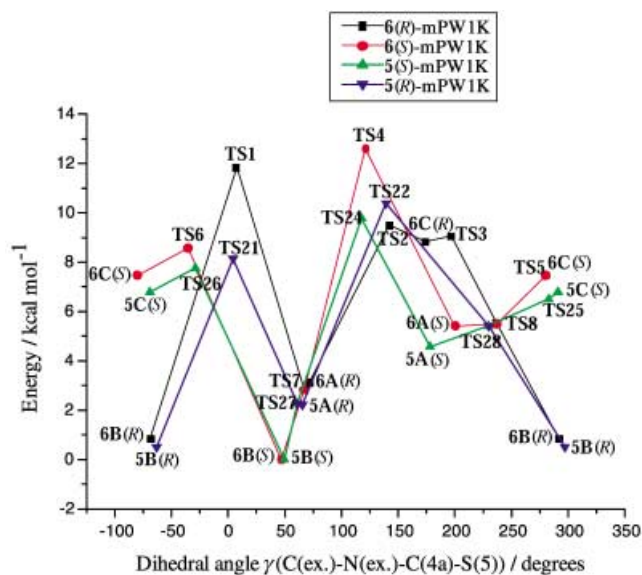


Figure 2. mPW1K/aug-cc-pvdz-calculated ZPE-corrected energy profiles for the model compounds **5** and **6**.

TS21, the rotational TS connecting **5B(R)** and **5A(R)**, is $8.1 \text{ kcal mol}^{-1}$ less stable than **5B(S)**. The corresponding activation barrier for **TS1** was $3.7 \text{ kcal mol}^{-1}$ higher. As observed for the neutral compound **6**, an inversion TS (**TS27**) is close in energy to the **5A(R)** isomer; this results

in an inversion process essentially without barrier. The inversion TS connects the **5A(R)** and **5B(S)** isomers. Further rotation from **5A(R)** leads to **TS22** (Figure 2). Attempts to find the **5C(R)** isomer, the assumed stable isomer going from **TS22**, always led to inversion to **5B(S)** or rotation to **5B(R)**. Thus, there are two different rotational TSs (**TS21** and **TS22**) connecting the **5A(R)** and **5B(R)** isomers, one by clockwise rotation and one by anticlockwise rotation, which are close in energy (8.1 and $10.4 \text{ kcal mol}^{-1}$, respectively).

Rotation of the amino group from the **5B(S)** isomer leads to **TS24** and requires $9.8 \text{ kcal mol}^{-1}$, which is $2.8 \text{ kcal mol}^{-1}$ less than for the corresponding **TS4**. The TS leads to the **5A(S)** isomer, which can interconvert to the **5C(S)** isomer via **TS25** (Figure 2). The PES in the vicinity of isomer **5C(S)** is very flat, and **5C(S)** is almost isoenergetic with **TS25**. **TS26** completes the rotational cycle connecting **5C(S)** and **5B(S)** and is $7.8 \text{ kcal mol}^{-1}$ less stable than **5B(S)**. The inversion TS **TS28** connects the **5B(R)** and **5A(S)** isomers and is $5.4 \text{ kcal mol}^{-1}$ less stable than **5B(S)**. Thus, the inversion process from **5A(S)** is essentially without barrier. Due to the low-barrier inversion processes in this system, formation of isomer **5A(R)** will take place from **5B(S)** rather than by amino group rotation. Similarly, the preferred formation of isomer **5A(S)** will be by inversion at N(ex.) rather than by amino group rotation. This means that the rate-determining TS for connecting all five stable cationic isomers is **TS26**, which has a ZPE-corrected activation barrier of $7.8 \text{ kcal mol}^{-1}$. This is slightly lower than the barrier calculated for the unchanged isomer **6**. When the N(ex.) lone pair interacts with the $\sigma^*[\text{C}(4a)-\text{N}(4)]$ orbital, the rotational barrier is slightly higher in cationic **TS22** than in uncharged **TS2**. This is an effect of stronger negative hyperconjugation in this direction in **5** than in **6**. Shortening of the C(4a)–N(ex.) bond in **TS22** (1.402 \AA) is greater than in **TS2** (1.436 \AA). This bond has in **TS22** an increased double-bond character as evidenced from the hybridisations (N(ex.): $\text{sp}^{1.8}$ and C(4a): $\text{sp}^{2.3}$) and thus a higher rotational barrier. The other optimised TSs have lower activation barriers in compound **5** than in compound **6**.

NBO analysis of cationic model compound 5: From the NBO analysis of cationic compound **5** (Table 5) it is evident that the

Table 5. Deletion energies (E_{del}) [kcal mol⁻¹], second-order perturbation energies ($E(2)$) [kcal mol⁻¹] and occupancy numbers (Occ.) [electrons] obtained from NBO analyses of isomers of compound **5** at the mPW1K/aug-cc-pvdz level of theory.

Isomer	$\sigma^*[\text{C}(4\text{a})-\text{S}(5)]$		$\sigma^*[\text{C}(4\text{a})-\text{N}(8)]$		$\sigma^*[\text{C}(4\text{a})-\text{N}(4)]$		$\sigma^*[\text{C}(\text{ex.})-\text{H}]$		N(ex.) lone pair Occ.	Sum of interactions $\Sigma E(2)$
	E_{del}	$E(2)$	E_{del}	$E(2)$	E_{del}	$E(2)$	E_{del}	$E(2)$		
5B(S)	19.82	22.16	5.99	6.96	–	1.06	7.55	7.50	1.859	44.12
5B(R)	19.61	21.65	–	2.85	2.90	3.67	8.00	7.89	1.868	42.20
5A(S)	–	1.74	19.55	21.86	4.31	5.51	8.43	8.32	1.874	43.78
5A(R)	5.06	6.10	18.48	20.69	–	1.24	8.07	8.02	1.869	43.38
5C(S)	4.74	5.72	–	0.70	20.70	25.06	9.00	8.94	1.869	46.74
TS21	–	3.30	5.73	6.66	12.52	14.95	8.12	8.00	1.891	40.09
TS22	8.06	9.80	–	< 0.5	16.20	20.40	9.26	9.26	1.866	47.26
TS24	4.38	5.21	–	4.32	12.65	15.14	7.60	7.49	1.890	39.56
TS25	8.51	10.33	–	< 0.5	18.14	22.82	9.13	9.18	1.860	49.37
TS26	–	< 0.5	8.11	9.29	13.92	16.98	8.50	8.41	1.880	41.04
TS27	12.78	15.80	16.10	18.94	–	< 0.5	7.79	8.01	1.838	51.46
TS28	12.05	14.79	14.42	16.96	–	< 0.5	8.22	8.40	1.850	51.41

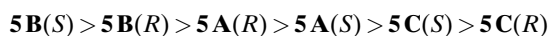
largest negative hyperconjugative effect is found in the **5C(S)** isomer, where the N(ex.) lone pair interacts with the antiperiplanar $\sigma^*[\text{C}(4\text{a})-\text{N}(4)]$ orbital. Removal of this interaction gives an estimated energy of 20.7 kcal mol⁻¹. As a comparison, the corresponding energy in **6C(S)** was estimated to be only 12.5 kcal mol⁻¹. The occupancy number of the N(ex.) lone pair in **5C(S)** was found to be 1.87, that is, 0.13 electrons occupy antibonding orbitals.

In isomer **5B(S)** the N(ex.) lone pair interacts mainly with the $\sigma^*[\text{C}(4\text{a})-\text{S}(5)]$ orbital and the strength of this interaction is calculated to be 19.8 kcal mol⁻¹. Thus in **5**, negative hyperconjugation from the N(ex.) lone pair is larger in the **C** isomer than in the **B** isomers. This opposes that observed in **6**, in which the thermodynamically most stable isomer also featured the strongest negative hyperconjugation effect. This is an effect of lowering of the orbital energy of the antibonding $\sigma^*[\text{C}(4\text{a})-\text{N}(4)]$ orbital upon protonation, leading to a reduced energy gap to the N(ex.)-lone pair orbital. The energy gap between the N(ex.)-lone pair orbital and the $\sigma^*[\text{C}(4\text{a})-\text{N}(4)]$ orbital is still larger than that between the N(ex.) lone pair orbital and the $\sigma^*[\text{C}(4\text{a})-\text{S}(5)]$ orbital, which has slightly increased on comparing **6** with **5** (see Supporting Information).

The negative hyperconjugation from the N(ex.) lone pair in isomers **5A(R)** and **5A(S)** is mainly directed to the C(4a)–N(8) bonds. The magnitudes of these delocalisations are calculated to be 4–5 kcal mol⁻¹ larger than those observed for isomers **6A**, mainly due to an increase in the Fock matrix elements. The strength of negative hyperconjugation ($\Sigma E(2)$) in **5** is ranked as follows:



while the following ordering results from the relative energies:

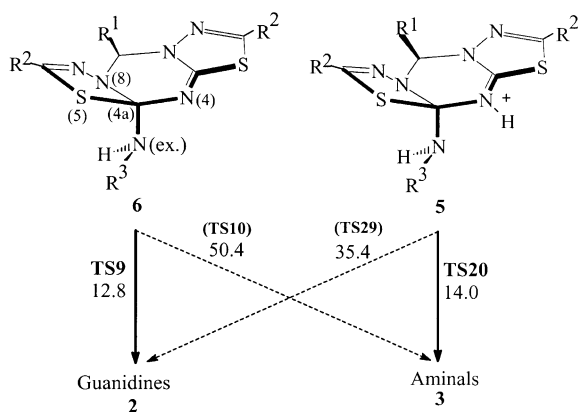


In **5A(S)** and **5C(S)** steric interactions are detected between the proton at C(9) and the proton at N(ex.) (in **5C(S)**) or a proton in the methyl group at N(ex.) (in **5A(S)**); these counterbalance the negative hyperconjugative effects.

The largest negative hyperconjugation in the cationic TSs are found in the inversion TS **TS27** (Table 5). In this TS, the

occupancy number of the N(ex.) lone pair is 1.84, thus 0.16 electrons occupy antibonding orbitals; the largest delocalisation found in this study. The interaction is largest in the C(4a)–S(5) and C(4a)–N(8) bonds. The largest $\Sigma E(2)$ value among the rotational TSs is found in **TS25**, which is also the rotational TS with the lowest activation barrier. On the other hand, in **TS22**, which is the least-stable rotational TS, the negative hyperconjugation is larger than, for instance, in the more stable **TS21** and **TS24**, although steric interaction are detected in all three of these (between the proton at C(9) and either the proton at N(ex.) (**TS21**) or a proton in the methyl group at N(ex.) (**TS22** and **TS24**)). This means that the strength of the negative hyperconjugation from N(ex.) is not proportional to the relative energies of the cationic TSs.

Ring-opening reactions: Analysing only the thermodynamic stabilities of the different isomers does not give an answer to the question of why a reaction channel via isomers **C** exists for the cationic compound **5** but not for the neutral compound **6**. The relative energies of isomers **C** compared with the most stable intermediate **B** is similar in the two cases: 6.8 kcal mol⁻¹ and 7.5 kcal mol⁻¹ in **5** and **6**, respectively. Our experimental observations, however, supported another explanation. For the uncharged compounds no formation of aminals was experimentally detected; this indicates that the TS for breaking the C(4a)–N(4) bond must be higher in energy than the TS for breaking the C(4a)–S(5) bond. There could be two reasons for this: the activation barrier for C(4a)–N(4)-bond cleavage is increased upon deprotonation or the activation barrier for C(4a)–S(5) bond cleavage decreases. To elucidate this, the different TSs were identified.^[56] The TS for C(4a)–S(5) bond cleavage, **TS9**, is calculated to be 12.8 kcal mol⁻¹ less stable than **6B(S)** at the mPW1K/aug-cc-pvdz level of theory (Scheme 5). The TS leads to a zwitterionic intermediate **7** that is more stable than isomer **6B(S)**.^[27] The TS for C(4a)–N(4) bond cleavage (**TS10**) on the other hand is 50.4 kcal mol⁻¹ less stable than the **6B(S)** isomer, and here bond breaking is concerted with proton transfer of the N(ex.) proton to the N(4) nitrogen. The barrier for C(4a)–N(4) bond cleavage of the cationic compound **5** is calculated to be 14.0 kcal mol⁻¹ (**TS20**) relative to **5B(S)**, while the TS **TS29** for breaking the C(4a)–S(5) bond is 35.4 kcal mol⁻¹ less stable



Scheme 5. mPW1K/aug-cc-pvdz-calculated activation barriers [kcal mol⁻¹] for the two reaction channels leading to guanidines **2** or aminals **3**. Solid lines are the favoured pathways, dashed lines the disfavoured pathways.

than **5B(S)**. In the latter TS, ring opening is concerted with proton transfer from N(4) to S(5) due to the increased basicity of the sulfur. Thus, upon protonation, the activation barrier for ring opening leading to the guanidine reaction channel is dramatically increased. This fits very well with the experimental findings. It should be kept in mind that the activation barriers for the TSs connecting all stable isomers of **5** or **6** were calculated to be lower than those for the ring-opening TSs, this means that the latter TSs are truly rate-determining.

A strong negative hyperconjugative effect, 72.1 kcal mol⁻¹, is calculated for **TS9** (Table 6). The dominating interaction is found between the N(ex.) lone pair and the σ^* [C(4a)–S(5)] orbital. Thus, this negative hyperconjugative stabilisation reduces the barrier of the ring-opening step by a significant amount. Similarly, in **TS20**, a very strong negative hyperconjugative stabilisation was discovered (Table 6). However, in this TS, the σ^* [C(4a)–N(4)] orbital and the N(ex.) lone pair interact. **TS29** features a smaller stabilisation from negative hyperconjugation than **TS20**, and no interaction between N(ex.) and σ^* [C(4a)–S(5)] could be detected in **TS10**.

Table 6. mPW1K/aug-cc-pvdz-calculated bond lengths [Å] and second-order perturbative estimates of negative hyperconjugative effects ($E(2)$) [kcal mol⁻¹] in different ring-opening TSs.

TS	Bond				σ^* [C(4a)–S(5)] $E(2)$	σ^* [C(4a)–N(4)] $E(2)$
	C(4a)–S(5)	C(4a)–N(4)	C(4a)–N(8)	C(4a)–N(ex.)		
TS9	2.420	1.376	1.394	1.348	72.14	1.73
TS29	2.080	1.430	1.443	1.348	61.46	–
TS10	1.728	2.474	1.343	1.340	0.84	–
TS20	1.774	1.914	1.398	1.350	0.85	73.72

From the data presented above, the experimental observations concerning the two reaction channels can be fully explained.

Conclusion

From this investigation we conclude that negative hyperconjugation may serve as a useful tool for controlling, in a predictable manner, the predominance of a specific interac-

tion pathway in a variety of closely related alternatives. In structures such as the intermediate compounds **5** (cationic) and **6** (uncharged), in which different σ^* -acceptor-bond orbitals compete for the interaction with the N(ex.)-nitrogen lone pair, calculation of the energetic gain from all interactions finally allows the evaluation of the predominant influence and a prediction of the most stable conformer. As such structure elements are present in many nucleophilic reaction pathways, we have addressed a central topic of organic chemistry in which an sp³-hybridised C atom is surrounded by four (different) hetero atoms, all of them capable of opening different reaction channels.

We choose salts **1** as starting materials as they are easily accessible and can be treated with a wide variety of nitrogen-based nucleophiles to immediately give the above-mentioned intermediates. Our experimental observation about the existence of two different reactions channels can now be explained on the basis of the theoretical investigations presented here. The procedures described here should serve as a reliable recipe to evaluate the reactivity pattern of related systems in which negative hyperconjugation dominates the formation of reactive intermediates and predominant products. Surprisingly, the reliable interpretation of the influence and importance of the negative hyperconjugation turns out to be much more complicated than we expected, not least because of the consequences of the well-known low inversion barrier of the N(ex.) centre. By the use of NBO analyses we demonstrated that the rough structural changes can be estimated by comparing the lengthening of the acceptor bond and shortening of the C(4a)–N(ex.) bond. Nevertheless, the overall effect of negative hyperconjugation is the result of contributions that stem from orbital interactions in different spatial directions. As shown for the most stable structure **6B(S)**, the σ^* orbital of the C(4a)–S(5) bond is the most important acceptor orbital, but there are contributions from σ^* [C(4a)–N(8)], σ^* [C(4a)–N(4)] and σ^* [C(ex.)–H] interactions as well. For isomers **6**, the relative stabilities parallel the strengths of the negative hyperconjugation. This causes significant elongation and weakening of the C(4a)–S(5) bond in **6B(S)**, which allows access to the zwitterionic species **7**.

Interestingly, this is not the case for the cationic species **5A–C**. Again, the most stable structure is **5B(S)**, here the σ^* [C(4a)–S(5)] bond orbital serves as acceptor orbital. However, the largest negative hyperconjugation (and a significantly elongated [C(4a)–N(4)] bond) was detected for isomer **5C(S)**, in which the N(ex.) lone pair interacts with the σ^* orbital of that bond. Evidently, formation of the less-energetic cationic isomers does not have consequences for any ring-opening reactions. Once isomer **5C(S)** is present (which is 6.8 kcal mol⁻¹ more energetic than **5B(S)**), the spontaneous C(4a)–N(4) bond cleavage becomes feasible and thus opens the pathway that yields aminals. Furthermore, our investigations indicate that the strength of

the negative hyperconjugation is more expressed in the cations **5** than in their uncharged counterparts **6** due to a smaller gap between the interacting orbitals in the former. It is noteworthy that significant negative hyperconjugative effects were also found in the transition structures responsible for the specific access to the two different reaction channels.

Such reactions, which are dominantly controlled by negative hyperconjugation and only to a lesser extent by the relative thermodynamic stability of structurally related isomers, deserve special interest and are part of our ongoing investigations.

Acknowledgement

S.O.N.L. gratefully acknowledges a postdoctoral stipend from the Wenner-Gren Foundation, Sweden. Financial support by the Deutsche Forschungsgemeinschaft (Sonderforschungsbereich 436) and by the Thüringer Ministerium für Wissenschaft, Forschung und Kultur (Erfurt, Germany) is gratefully acknowledged. We thank Dr. M. Walther and Dr. K. Wermann for useful discussions. A. Wallman is acknowledged for valuable suggestions to the manuscript.

- [1] M. Adler, M. Marsch, N. S. Nudelman, G. Boche, *Angew. Chem.* **1999**, *111*, 1345; *Angew. Chem. Int. Ed.* **1999**, *38*, 1261.
- [2] R. W. Alder, T. M. G. Carniero, R. W. Mowlam, A. G. Orpen, P. A. Petillo, D. J. Vachon, G. R. Weisman, J. M. White, *J. Chem. Soc. Perkin Trans. 2* **1999**, 589.
- [3] C. J. Cramer, D. G. Truhlar, A. D. French, *Carbohydr. Res.* **1997**, *298*, 1.
- [4] C. J. Cramer, A. M. Kelterer, A. D. French, *J. Comput. Chem.* **2001**, *22*, 1194.
- [5] B. Y. Ma, H. F. Schaefer III, N. L. Allinger, *J. Am. Chem. Soc.* **1998**, *120*, 3411.
- [6] P. A. Petillo, L. E. Lerner in *The Anomeric Effect and Associated Stereoelectronic Effects*, Vol. 539 (Ed.: G. R. J. Thatcher), American Chemical Society, Washington DC, **1993**, p. 156.
- [7] U. Salzner, P. v. R. Schleyer, *J. Org. Chem.* **1994**, *59*, 2138.
- [8] D. Suarez, T. L. Sordo, J. A. Sordo, *J. Am. Chem. Soc.* **1996**, *118*, 9850.
- [9] N.-B. Wong, Y.-S. Cheung, D.-Y. Wu, Y. Ren, A. Tian, W.-K. Li, *J. Phys. Chem. A* **2000**, *104*, 6077.
- [10] E. Juaristi, *Introduction to Stereochemistry and Conformational Analysis*, Wiley, New York, **1991**.
- [11] P. Deslongchamps, *Stereoelectronic Effects in Organic Chemistry*, Pergamon, Oxford, **1984**.
- [12] F. Uehara, M. Sato, C. Kaneko, H. Kurihara, *J. Org. Chem.* **1999**, *64*, 1436.
- [13] R. Koch, E. Anders, *J. Org. Chem.* **1994**, *59*, 4529.
- [14] R. Koch, E. Anders, *J. Org. Chem.* **1995**, *60*, 5861.
- [15] I. V. Alabugin, *J. Org. Chem.* **2000**, *65*, 3910.
- [16] J. E. Anderson, *J. Org. Chem.* **2000**, *65*, 748.
- [17] P. v. R. Schleyer, A. J. Kos, *Tetrahedron* **1983**, *39*, 1141.
- [18] A. E. Reed, P. v. R. Schleyer, *J. Am. Chem. Soc.* **1990**, *112*, 1434.
- [19] K. Nordhoff, E. Anders, *J. Org. Chem.* **1999**, *64*, 7485.
- [20] N. K. Banavali, A. D. MacKerell, Jr., *J. Am. Chem. Soc.* **2001**, *123*, 6747.
- [21] P. R. Schreiner, *Angew. Chem.* **2002**, *114*, 3729; *Angew. Chem. Int. Ed.* **2002**, *41*, 3579.
- [22] V. Pophristic, L. Goodman, *Nature* **2001**, *411*, 565.
- [23] E. Anders, K. Wermann, B. Wiedel, W. Günther, H. Görls, *Eur. J. Org. Chem.* **1998**, 2923.
- [24] K. Wermann, M. Walther, W. Günther, H. Görls, E. Anders, *J. Org. Chem.* **2001**, *66*, 720.
- [25] M. Walther, K. Wermann, H. Görls, E. Anders, *Synthesis* **2001**, 1327.
- [26] K. Wermann, M. Walther, E. Anders, *Arkivoc* **2002**, [http://www.arkat-usa.org/arkjournal/2002/Part\(x\) General/2-532F/2-532F.htm](http://www.arkat-usa.org/arkjournal/2002/Part(x) General/2-532F/2-532F.htm), 24.
- [27] K. Wermann, M. Walther, W. Günther, H. Görls, E. Anders, *Eur. J. Org. Chem.* **2003**, 1389. Protonation at the N(7) or the N(8) position results in intermediates that, at the mPW1K/aug-cc-pvdz level of theory, are calculated to be 11.8 and 18.2 kcal mol⁻¹, respectively, less stable than the N(4)-protonated tautomer.
- [28] In the cationic model system **5** we used R¹ = R² = R³ = CH₃, while in the uncharged model system **6** R¹ = R² = H, R³ = CH₃ was used in order to save computer time. The methyl groups in **5** were chosen on behalf of their electron-donating effect that will stabilise the cation.
- [29] Gaussian 98 (Revision A.11.4), M. J. Frisch, G. W. Trucks, H. B. Schlegel, G. E. Scuseria, M. A. Robb, J. R. Cheeseman, V. G. Zakrzewski, J. A. Montgomery Jr., R. E. Stratmann, J. C. Burant, S. Dapprich, J. M. Millam, A. D. Daniels, K. N. Kudin, M. C. Strain, O. Farkas, J. Tomasi, V. Barone, M. Cossi, R. Cammi, B. Mennucci, C. Pomelli, C. Adamo, S. Clifford, J. Ochterski, G. A. Petersson, P. Y. Ayala, Q. Cui, K. Morokuma, P. Salvador, J. J. Dannenberg, D. K. Malick, A. D. Rabuck, K. Raghavachari, J. B. Foresman, J. Cioslowski, J. V. Ortiz, A. G. Baboul, B. B. Stefanov, G. Liu, A. Liashenko, P. Piskorz, I. Komaromi, R. Gomperts, R. L. Martin, D. J. Fox, T. Keith, M. A. Al-Laham, C. Y. Peng, A. Nanayakkara, M. Challacombe, P. M. W. Gill, B. Johnson, W. Chen, M. W. Wong, J. L. Andres, C. Gonzalez, M. Head-Gordon, E. S. Replogle, J. A. Pople, Gaussian, Inc., Pittsburgh PA, **2001**.
- [30] E. D. Glendenning, J. K. Badenhoop, A. E. Reed, J. E. Carpenter, J. A. Bohmann, C. M. Morales, F. Weinhold, *NBO 5.0*, Theoretical Chemistry Institute, University of Wisconsin, Madison, **2001**.
- [31] A. D. Becke, *J. Chem. Phys.* **1993**, *98*, 5648.
- [32] C. Lee, W. Yang, R. G. Parr, *Phys. Rev. B: Condens. Matter Mater. Phys.* **1988**, *37*, 785.
- [33] C. Adamo, V. Barone, *J. Chem. Phys.* **1998**, *108*, 664.
- [34] J. P. Perdew in *Electronic Structure of Solids '91* (Eds.: P. Ziesche, H. Eschrig), Akademie Verlag, Berlin, **1991**, p. 11.
- [35] B. J. Lynch, P. L. Fast, M. Harris, D. G. Truhlar, *J. Phys. Chem. A* **2000**, *104*, 4811.
- [36] B. J. Lynch, D. G. Truhlar, *J. Phys. Chem. A* **2001**, *105*, 2936.
- [37] B. J. Lynch, D. G. Truhlar, *J. Phys. Chem. A* **2002**, *106*, 842.
- [38] C. Møller, M. S. Plesset, *Phys. Rev.* **1934**, *46*, 618.
- [39] G. E. Scuseria, H. F. Schaefer III, *J. Chem. Phys.* **1989**, *90*, 3700.
- [40] R. Krishnan, J. S. Binkley, R. Seeger, J. A. Pople, *J. Chem. Phys.* **1980**, *72*, 650.
- [41] T. Clark, J. Chandrasekhar, G. W. Spitznagel, P. v. R. Schleyer, *J. Comput. Chem.* **1983**, *4*, 294.
- [42] G. W. Spitznagel, T. Clark, J. Chandrasekhar, P. v. R. Schleyer, *J. Comput. Chem.* **1982**, *3*, 363.
- [43] J. Chandrasekhar, J. G. Andrade, P. v. R. Schleyer, *J. Am. Chem. Soc.* **1981**, *103*, 5609.
- [44] T. H. Dunning, *J. Chem. Phys.* **1989**, *90*, 1007.
- [45] R. A. Kendall, T. H. Dunning, R. J. Harrison, *J. Chem. Phys.* **1992**, *96*, 6796.
- [46] K. Fukui, *Acc. Chem. Res.* **1981**, *14*, 363.
- [47] C. A. Gonzalez, H. B. Schlegel, *J. Chem. Phys.* **1989**, *90*, 2154.
- [48] C. A. Gonzalez, H. B. Schlegel, *J. Phys. Chem.* **1990**, *94*, 5523.
- [49] P. Y. Ayala, H. B. Schlegel, *J. Chem. Phys.* **1997**, *107*, 375.
- [50] A. E. Reed, R. B. Weinstock, F. Weinhold, *J. Chem. Phys.* **1985**, *83*, 735. The accuracy of the absolute values of the delocalisation energies are not known and should therefore be interpreted with care but it is discussed that the calculated relative energies are valid to use.^[3] The magnitude of the absolute values is about 20 kcal mol⁻¹, which is similar to the magnitude of the delocalisations calculated for the phosphodiester backbone.^[20] Details regarding the DEL procedure in the NBO analysis can be found in F. Weinhold in *Encyclopedia of Computational Chemistry* (Ed.: P. v. R. Schleyer), Wiley, Chichester, **1998**, p. 1805, in ref. [2] and the references cited therein, in ref. [7] and at http://www.chem.wisc.edu/~nbo5/tut_del.htm.
- [51] The steric interactions were detected by identification of H-H bond lengths smaller than the sum of the van der Waals radius of two hydrogen atoms (2.40 Å).^[52]
- [52] A. Bondi, *J. Phys. Chem.* **1964**, *88*, 441.
- [53] The E(2) estimation is performed at a default NBO-calculation by using Gaussian 98 while E_{del} requires an additional calculation. In Equation (1) below describing the E(2) estimation, n_{lp} is the occupancy number of the lone pair, F_{ij} the Fock matrix element

between orbitals i and j , and $\Delta\epsilon$ is the energy gap between the two interacting orbitals:

$$E(2) = -n_{\text{lp}} \frac{F_{ij}^2}{\Delta\epsilon} \quad (1)$$

[54] I. V. Alabugin, T. A. Zeidan, *J. Am. Chem. Soc.* **2002**, *124*, 3175.

[55] It is interesting to note that the interaction between the N lone pair and the $\sigma^*[\text{C}(\text{ex.})\text{-H}]$ orbital of the methyl group also is rather large, only 2–3 kcal mol⁻¹ smaller than the interaction involving the

$\sigma^*[\text{C}(4\text{a})\text{-N}(4)]$ orbital. It is easy to imagine that a more polarised R group on N(ex.) will give a stronger effect.

[56] For compound **6**, isomer **6B** was used as the starting point for localisation of **TS9**, and isomer **6C** was used for localisation of **TS10**. For compound **5**, isomer **5B** was used as the starting point for localisation of **TS29**, and isomer **5C** was used for localisation of **TS20**.

Received: February 24, 2003 [F4878]